Environmental Science & Technology

Article

pubs.acs.org/est

Dynamic Exergy Method for Evaluating the Control and Operation of Oxy-Combustion Boiler Island Systems

Bo Jin,[†,‡] Haibo Zhao,[*,†] Chuguang Zheng,[†] and Zhiwu Liang[‡]

[†]State Key Laboratory of Coal Combustion, School of Energy and Power Engineering, Huazhong University of Science and Technology, Luoyu Road 1037, Wuhan, Hubei 430074, P. R. China

[‡]Joint International Center for CO_2 Capture and Storage (iCCS), Provincial Key Laboratory for Cost-Effective Utilization of Fossil Aimed at Reducing Carbon Dioxide Emissions, College of Chemistry and Chemical Engineering, Hunan University, Changsha, Hunan 410082, P. R. China

Supporting Information

ABSTRACT: Exergy-based methods are widely applied to assess the performance of energy conversion systems; however, these methods mainly focus on a certain steady-state and have limited applications for evaluating the control impacts on system operation. To dynamically obtain the thermodynamic behavior and reveal the influences of control structures, layers and loops, on system energy performance, a dynamic exergy method is developed, improved, and applied to a complex oxy-combustion boiler island system for the first time. The three most common operating scenarios are studied, and the results show that the flow rate change process leads to less energy consumption than oxygen purity and air in-leakage change processes. The variation of oxygen purity produces the largest impact on system operation, and the operating parameter sensitivity is not affected by the presence of process control. The control system saves energy during flow rate and oxygen purity change processes, while it consumes energy during the air in-leakage change process. More attention should be paid to the oxygen purity change because it requires the largest control cost. In the control system, the supervisory control layer requires the greatest energy consumption and the largest control cost to maintain operating targets, while the steam control loops cause the main energy consumption.

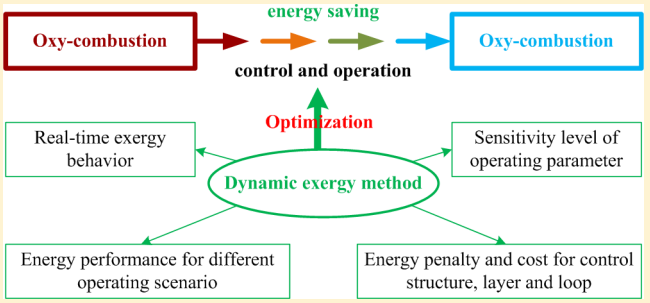

1. INTRODUCTION

The energy conversion process, as an essential procedure for energy supply in society, transforms natural resources into useful products. To understand the characteristics of the process, exergy-based approaches are commonly applied to assess the thermodynamic performance, economic properties, environmental impacts, and sustainable developments.[1,2] Exergy analyses[3,4] aim to find the source of thermodynamic irreversibility, while a theory of exergy cost[5] is formed to determine the fuel consumption required to gain the products. When monetary cost is further considered, a thermoeconomic cost analysis[6,7] is proposed to interpret the cost formation process. The anomalies are detected, quantified, and located by a thermoeconomic diagnosis,[8] while the optimal design and operation are obtained through thermoeconomic optimization.[9] By further combining the emergy analysis, the ecological cumulative exergy consumption (ECEC)[10] is expanded to account for natural contributions to industrial activities. Inspired from an exergetic life cycle assessment (ELCA),[11] an exergoenvironmental analysis[12,13] is proposed to identify and find the options to reduce the environmental impacts. However, these exergy-based methods could not identify system performance in real-time because a certain steady-state rather than the dynamic operating conditions is adopted for evaluation. Actually, the thermodynamic behavior is time-dependent when the system operating condition changes as a result of the operating command, disturbance, and emergency condition under control interventions. In addition, limited attention is paid to the use of exergy-based methods for investigating the control impacts on energy performance during system operations. Therefore, useful methods should be developed to obtain the dynamic exergy behavior, assess the control impacts simultaneously, and, more importantly, provide guidelines for achieving energy efficient operations.

Fortunately, some efforts have been made to promote these understandings. Derived from dynamic exergy balance, Luyben et al.[14] defined a system response time to measure the relationship between process control and thermodynamics. Munir et al.[15] presented an exergy eco-efficiency factor to determine the desirable control pairings and then used a dynamic exergy plot[16] to validate the corresponding result. In these works, the exergy parameters were calculated from steady-state simulation results, and the defined exergy

Received: August 13, 2016
Revised: November 30, 2016
Accepted: November 30, 2016
Published: November 30, 2016

DOI: 10.1021/acs.est.6b04096
Environ. Sci. Technol. 2017, 51, 725−732

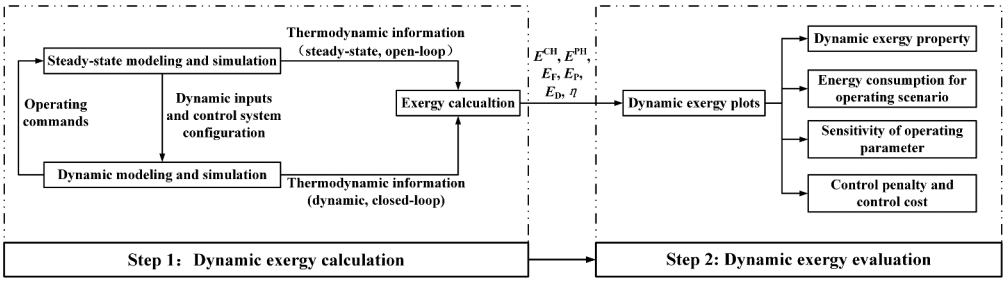

Figure 1. Systematic procedures for implementing the dynamic exergy method.

evaluation factor was limited to compare different control strategies. To overcome these issues, Jin et al.[17] proposed a systematic dynamic exergy method and successfully applied the method to a CO_2 compression and purification unit, where dynamic information for the thermodynamic performance and control impacts were identified. However, the entire control system rather than the internal structures in the control system was evaluated in the dynamic exergy method. Thus, the approach still needs improvement to determine the energy performance influences of control layers and loops in the control system, and its applications should be further examined for more complex energy conversion systems.

Oxy-combustion, a complex energy conversion system, is considered as a promising CO_2 capture option to reduce CO_2 emissions from power plants. It can be retrofitted from a conventional power plant with minor modifications[18,19] even though additional energy penalties[20,21] and economic costs[22,23] are required. To realize its commercial demonstration, great efforts have been made to design a suitable control system[24] and obtain dynamic behavior.[24,25] Nevertheless, it is still required to seek new methodology to reduce energy consumption. This study presents a novel approach to achieve energy conservation through optimizing the control and operation of an oxy-combustion boiler island system and confirms the application of a dynamic exergy method for complex energy conversion systems.

This paper discusses the following: (1) a dynamic exergy method is developed to evaluate the real-time thermodynamic performance and quantify the control impacts on system operations on the viewpoint of thermodynamics; (2) the method is further improved by introducing an energy utilization ratio and uncovering the energy performance and cost for control layers and loops in the control system; (3) the method is applied for the first time to a complex oxy-combustion boiler island system. This study offers a powerful tool to design a thermodynamically efficient and environmentally friendly system.

2. METHODOLOGY: DYNAMIC EXERGY METHOD

The dynamic exergy concept is the main technique used to interpret the dynamic exergy method: every exergy parameter has a specific value and is used to reflect the thermodynamic characteristics of a system at every time point (t). To describe the real-time thermodynamic behavior for an open system, the dynamic exergy balance is presented below[3,14]

$$\frac{dE(x(t))}{dt} = \left(\sum_{in} \dot{m}_{in} e_{in} - \sum_{out} \dot{m}_{out} e_{out}\right) + \sum_{i} (T_i - T_0)/T_i \dot{Q}_i - \left(\dot{W} - p_0 \frac{dV}{dt}\right) - T_0 \dot{\sigma}(x(t)) \quad (1)$$

where the left term represents the exergy change rate, the first three right terms represent the exergy transfer rates through fluid streams, heat transfer, and mechanical work, and $\dot{\sigma}(x(t))$ indicates total entropy production rate. From the above equation, exergy flows at t and t+dt appear with a difference dE when the system operates unsteadily, while the exergy flows are identical under steady-state operation. Calculating these exergy flows at every time point is used to determine the dynamic exergy plots, which can be used to compare different operating scenarios, quantify the energy consumptions for operating conditions, and identify the influences of control structures, layers and loops on system operation. To identify these dynamic exergy features, a systematic dynamic exergy method[17] (Figure 1) is developed and improved to provide useful information for achieving thermodynamically efficient operations.

2.1. Dynamic Exergy Calculation. This procedure aims at implementing the exergy parameter calculations for different operating scenarios to obtain the real-time exergy curves. First, a steady-state model is developed and validated by comparing steady-state simulation results with actual plant design data. Dynamic inputs are used to transform the steady-state model into a dynamic model when dynamic simulation preparations[26−28] are completed. Then, dynamic simulations are conducted by configuring a designed closed-loop control system. When the operating commands are applied, the thermodynamic information (flow rate, temperature, pressure, composition, enthalpy, and entropy) at every time point for the closed-loop and open-loop (i.e., without control system) controlled systems during different operating scenarios is determined from the dynamic and steady-state simulation results, respectively. Finally, the dynamic and steady-state thermodynamic information is imported into the exergy calculation program to calculate the required exergy parameters for forming dynamic exergy curves. In the exergy calculation, the physical exergy (E^{PH}), chemical exergy (E^{CH}), fuel exergy (E_F), product exergy (E_P), exergy destruction (E_D), and exergy efficiency (η) are considered, and their definitions, equations,[3,20,22] and reference environment state[29] are explained in Text S3.

2.2. Dynamic Exergy Evaluation. The main goal of the dynamic exergy evaluation is to assess the control and operation of the studied system using the following defined indicators. At the beginning, the dynamic exergy property for characterizing the real-time thermodynamic behavior is obtained from the dynamic exergy plots. Calculated from eq 2, the energy inputs, outputs, and consumptions for different operating cases at a certain time period are determined by counting areas under the dynamic fuel exergy, product exergy, and exergy destruction curves

DOI: 10.1021/acs.est.6b04096
Environ. Sci. Technol. 2017, 51, 725−732

$$\varphi_i = \int_{t_0}^{t_1} E_i(t)\mathrm{d}t \tag{2}$$

where φ is energy (kW·h), t is time point, subscripts "0" and "1" illustrate the initial and final time points, and i represents the above types of exergy parameters. Then, the energy utilization ratio (λ), defined as the ratio of energy outputs to energy inputs, can be used to justify whether the control system saves or consumes energy when comparing the value under open-loop control with that in closed-loop control during operating conditions. A control system would realize energy savings when this parameter in a closed-loop control is larger than that in open-loop control; in the opposite situation, the control system consumes energy.

Based on the variations of energy consumptions and operating inputs, a sensitivity factor is introduced to evaluate the sensitivity levels of operating parameters on system operation

$$\beta = \left| \left(\frac{d\varphi_D}{\varphi_{D,0}} \right) / \left(\frac{du}{u_0} \right) \right| \tag{3}$$

where β is a nondimensional number, $d\varphi_D$ represents the amount of energy consumption that generated during the time period from giving command to reaching the final steady-state, $\varphi_{D,0}$ is the produced energy consumption if the initial operating condition lasts for the above time period, u is the variable used to complete the operating command, and u_0 is the initial value of u. The larger sensitive factor causes greater fluctuations during system operation when the corresponding operating parameters change.

Control penalty, defined as the difference between open-loop control and control systems with different control structures with regard to energy consumption, justifies the effects of control structure, layers and loops on system performance. Through acquiring simultaneously energy consumption under all control systems, the control penalty can be calculated by the equation shown below

$$\Delta\varphi_j = \varphi_{D\_j} - \varphi_{D\_open} \tag{4}$$

where j represents the control system with different control layers and loops, and the sign of $\Delta\varphi_j$ reveals the role the control system plays in energy saving (i.e., "−") or energy dissipation (i.e., "+"). Therefore, the inherent energy performance for control layers and loops in the control system can be uncovered to judge their contributions to system thermodynamic characteristics and to optimize control structures for reducing energy consumption.

Analogizing the cost of control system on thermoeconomic diagnosis,[30] the control cost is defined as the ratio of the total fuel impact to the total product impact in the form of absolute value

$$k_j = \left| \frac{\varphi_{F\_j} - \varphi_{F\_open}}{\varphi_{P\_j} - \varphi_{P\_open}} \right| \tag{5}$$

where the numerator equals the difference between two energy inputs, while the denominator is the difference between two energy outputs under the closed-loop control systems with different structures and open-loop control. The physical meaning of this variable lies in quantifying the demand of control effort to achieve the desirable product quality when fuel input is no longer equal to the specified value. This change indicates that more attention should be paid to an operating parameter if the corresponding control cost is larger. For control structures, the value can also be used to manifest the important extent of control layers and loops during certain operating scenarios.

3. RESULTS AND DISCUSSION

To validate the dynamic exergy method, a complex oxy-combustion boiler island system[24,25] (shown in Figure S1) is used, and the description for the process flow diagram is presented in Text S1.

3.1. Steady-State Modeling and Simulation. Based on previous studies,[24,25] a steady-state model for an oxy-combustion boiler island is developed by Aspen Plus. The modeling assumptions, key boundary conditions, and coal composition are summarized in Text S2, Table S1, and Table S2, respectively, to accomplish the steady-state simulation. Then, three operating commands of flow rate ramp, oxygen purity ramp, and air in-leakage step changes are put into steady-state simulation to gain the thermodynamic information under free conditions (no control is configured in the system). The first case means that system load ramps at a rate of 2%/min from 100% to 80%, the second case illustrates that oxygen supplying purity ramps at a rate of 0.2%/min from 95 mol % to 99 mol %, and the last case represents that 50% step increase of air in-leakage flow rate from the boiler is applied.

3.2. Dynamic Modeling and Simulation. As presented in previous studies,[24,25] a dynamic model for the oxy-combustion boiler island is then imported into the Aspen Plus Dynamics when the required dynamic preparations are completed. As illustrated in Figure S1 and described in Text S1, a closed-loop control system is installed in the analyzed system to implement automatic operation and maintain the desirable conditions. Flow controls and furnace pressure control are presented in a regulatory control layer to achieve stabilization and local disturbance rejection, while main steam temperature control (TC_SH), reheat steam temperature control (TC_RH), ratio controls, and flue gas O_2 content control (CC_O_2) are considered in the supervisory control layer to realize reasonable steam temperatures and a desirable combustion process. Then, identical operating commands as mentioned above are entered into the dynamic model to obtain the corresponding thermodynamic information in real-time under constrained conditions (closed-loop control).

3.3. Exergy Calculation. Calculated from eqs S1−S6, the components and distributions for fuel and product exergies are presented in Figure S2. The exergies for coal, oxygen, feedwater, reheat extraction, reheat steam spray water, and fan power consumptions are included in fuel exergy, while product exergy consists of the exergies of main steam, reheat steam, and flue gas entering into the CPU. Then, exergy destruction and exergy efficiency for the oxy-combustion boiler island configured with a closed-loop control system at the initial operating state are determined as 1462.41 MW and 55.83%, respectively. Finally, the dynamic exergy curves varying with time for the oxy-combustion boiler island under different control structures and different operating conditions are obtained for the dynamic exergy evaluation.

3.4. Dynamic Exergy Property. *3.4.1. Flow Rate Ramp Change Case.* Dynamic exergy properties for the oxy-combustion boiler island during the flow rate change process are shown in Figure 2 (large, clear pictures are presented in

DOI: 10.1021/acs.est.6b04096
Environ. Sci. Technol. 2017, 51, 725−732

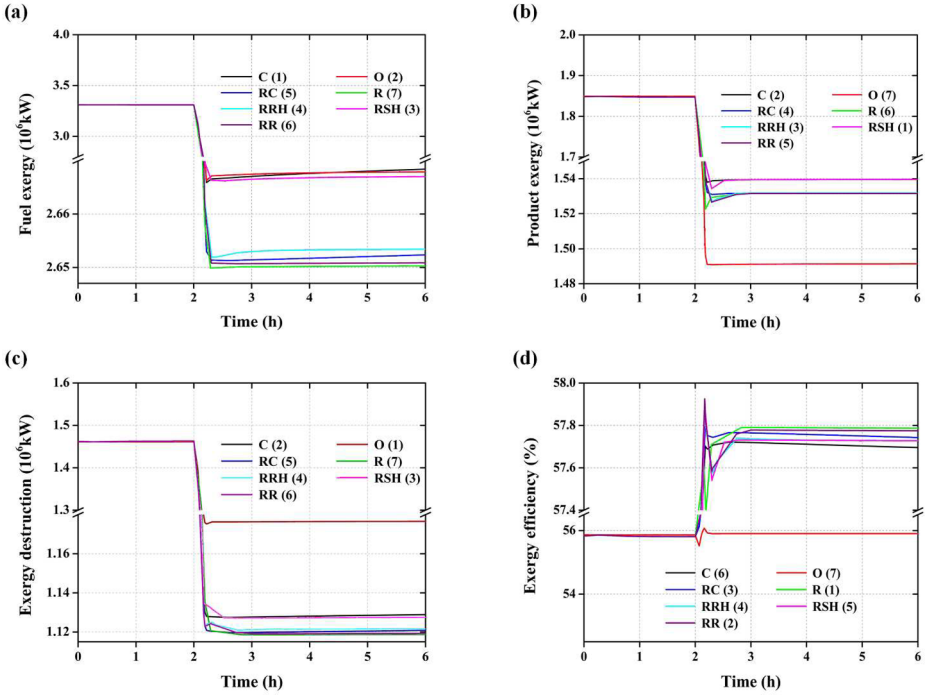

Figure 2. Dynamic exergy property for oxy-combustion boiler island under the flow rate ramp change case: (a) fuel exergy, (b) product exergy, (c) exergy efficiency, and (d) exergy destruction.

Figure S3), in which the numbers behind the control structures are used to justify the magnitude of the final state parameters. To distinguish between the different control structures, the following abbreviations are defined: open-loop control (**O**), closed-loop control + open-loop control (**C**), regulatory control layer + open-loop control (**R**), regulatory control layer + ratio controls + open-loop control (**RR**), regulatory control layer + ratio controls + reheat steam temperature control + open-loop control (**RRH**), regulatory control layer + ratio controls + main steam temperature control + open-loop control (**RSH**), and regulatory control layer + ratio controls + flue gas O_2 content control + open-loop control (**RC**). During this operating process, the flow rate variation plays the main role in the evolutions of fuel and product exergies. The unchanged unit physical exergy and unit chemical exergy result in the change of fuel exergy because composition, pressure, and temperature for these input flows are constant. However, two factors contribute to the product exergy variation. The first factor is that the steam exergy is larger than that of the flue gas even though the steam and flue gas conditions are variable. Another factor is that flow rate leads to stronger effects on the steam exergy than that of temperature and pressure.

In Figure 2(a), the difference between **O** and **R** comes from real-time power consumption changes from fans and stream exergies caused by flow controls and furnace pressure control. Due to the feedforward action derived from ratio control between coal and oxygen, the exergy of the oxygen and power consumptions from PA and FD in **RR** are larger than those in **R**, mainly caused by the larger variation of oxygen exergy. The fuel exergy in **RC** is greater than that in **RR**, which is attributed to the larger increment of power consumption from PA and FD, even though its oxygen exergy decreases when the control action from CC_O_2 contributes to decreases in the oxygen flow rate and pressure. The TC_RH control action leads to a spray water flow rate increase for moderating reheat steam temperature; thus, a larger fuel exergy is observed in **RRH** when compared to that in **RR**. Similarly, the spray water flow rate increase for moderating the main steam temperature is derived from the TC_SH control action, which then gives the result that the fuel exergy in **RSH** is larger than that in **RR**. Among the analyzed control structures, the fuel exergy in **C** is maximum. When compared to that in **R**, it is ascribed to the comprehensive control actions from the supervisory control layer (especially TC_SH), which results in the augments of spray water flow rate and fan power consumptions.

Figure 2(b) illustrates that the product exergies of **RR** and **R** are different, based on the control actions of the ratio controls, which bring the phenomenon that the main steam and reheat steam temperatures in **RR** are slightly higher than those in **R**. In **RC**, CC_O_2 causes the CO_2 concentration in flue gas to decrease linearly,[24] and its value is higher than that in **RR** from the time of giving command to the final state. Therefore, the exergy of the flue gas in **RC** is larger than that in **RR**. However, CC_O_2 leads to a smaller exergy value of steam because the combustion fluctuation in the furnace contributes to lower values for main and reheat steam temperatures in **RC**. Compared with the variations of exergy for flue gas and steam, it is found that the exergy increment for flue gas (+302.96 kW) is larger than the exergy increase for steam (−288.84 kW); therefore, the product exergy in **RC** is larger than that in **RR**. Compared to **RRH** and **RR**, the reheat steam exergy in **RRH** increases roughly 1715.27 kW because TC_RH forces the reheat steam temperature back to its set point by increasing the corresponding spray water flow rate. The main steam exergy decreases roughly 1456.91 kW because the main steam temperature decreases, as resulted from the staggered reheater and superheater arrangements. Therefore, the product exergy of **RRH** is larger than that of **RR**, and the exergy of flue gas in **RRH** equals that in **RR**. In a similar way, TC_SH in **RSH** maintains the main steam temperature around its set point by

DOI: 10.1021/acs.est.6b04096
Environ. Sci. Technol. 2017, 51, 725−732

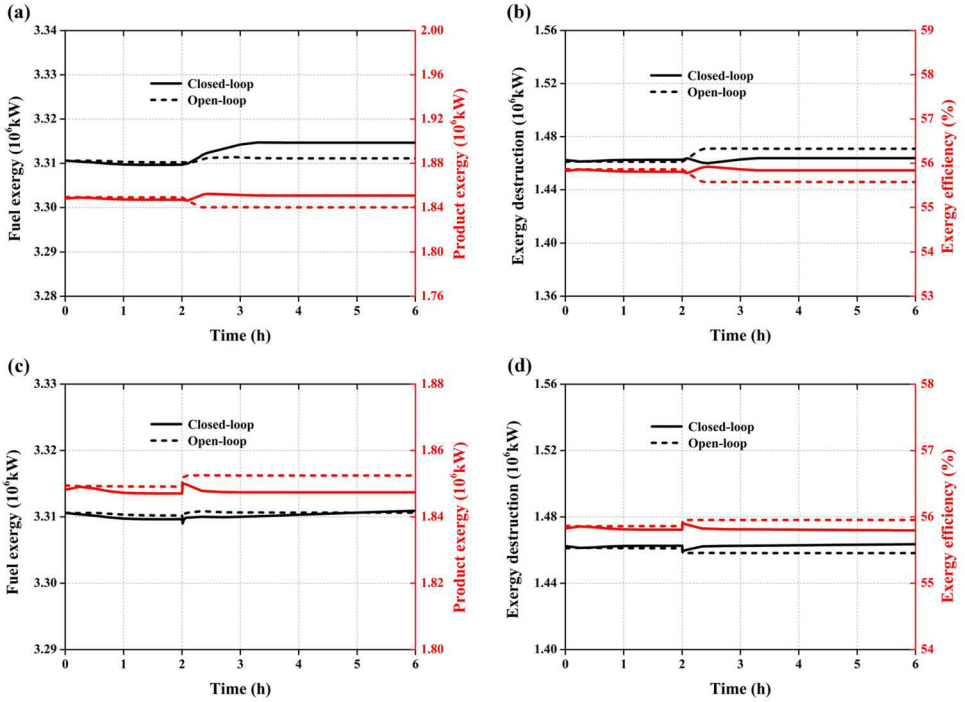

Figure 3. Dynamic exergy properties for oxy-combustion boiler island under oxygen purity ramp change (a and b) and air in-leakage step change (c and d) cases.

increasing the spray water flow rate from double stages spray attemperators, which then leads to a decrease in the reheat steam temperature. Hence, the main steam exergy increases approximately 1.79%, while the reheat steam exergy decreases approximately 1.02% in **RSH** in comparison with those in **RR**. Thus, the product exergy of **RSH** is larger than that of **RR** due to their identical flue gas exergy. In contrast with the product exergy in **R**, the product exergy of **C** is larger because the comprehensive actions from the supervisory control layer increase the amount of spray water to maintain steam temperatures and CO_2 concentration in the flue gas. This means that the main steam exergy increases approximately 1.78%, the reheat steam exergy decreases approximately 1.05%, and the flue gas exergy increases approximately 0.43%.

As the final state in Figures 2(c) illustrates, **O** accounts for the maximum exergy destruction because its fuel exergy ranks second and its product exergy is minimum. The minimum exergy occurs in **R** because of its decreased fuel exergy and variation that is larger than that of the product exergy. The largest exergy destruction in **O** reveals that exergy consumption for the system is determined by the plant configuration and device characteristics. Moreover, to satisfy the control targets and safe operation, exergy consumption is necessary for the control system. As observed from Figure 2(d), the exergy efficiency in **C** changes slightly, while the exergy efficiencies for other control strategies increase almost linearly. The main reason for different exergy parameters at the final state is that different control strategies make the system approach to different control targets and operating parameters.

3.4.2. Oxygen Purity Ramp Change Case. Figure 3(a) illustrates that the fuel exergy under closed-loop control increases approximately 0.12% because the robust control actions are imposed on the spray water, flue gas, and fans. As the furnace combustion performance is enhanced when elevating the oxygen purity, more spray water is required to realize the steam temperature control objectives. Thus, the spray water exergies for TC_SH and TC_RH increase roughly 1.26% and 2.08%, respectively. Meanwhile, the flow and pressure controls cause approximately 2.37% more fan power consumptions, even though the oxygen exergy decreases nearly 1.60% because CC_O_2 gives rise to decreased oxygen flow rate and pressure. The product exergy under closed-loop control increases approximately 0.14% because the spray water increment moderated by the steam temperature controls increases the steam exergies (+0.04% for reheat steam and +0.06% for main steam) and the CO_2 concentration increase in flue gas resulted from CC_O_2[24] increases in the flue gas exergy (+2.37%). As shown in Figure 3(b), the exergy destruction and exergy efficiency increase by 0.09% and 0.02%, respectively. These results are derived from the interactions between the fuel exergy and product exergy, which means the amount of fuel exergy increase (+4060.90 kW) is larger than that of the product exergy (+2673.97 kW), and the extent of variation for fuel exergy (+0.12%) is smaller than that of product exergy (+0.14%). Due to the real-time regulations from the closed-loop control system, a different dynamic exergy performance for open-loop control is observed and discussed in Text S4.

3.4.3. Air in-Leakage Step Change Case. Two main factors impact the fuel exergy (Figure 3(c)) under closed-loop control with a step increase. First, the exergies of the main steam and reheat steam increase approximately 0.10% and 0.28%, respectively, because more spray water is needed for matching the control goals of steam temperatures when enhanced combustion occurs along with external oxygen entering the furnace. Additionally, due to the variation of flue gas parameters, fan power consumption increases roughly 5.12%, even though the oxygen exergy decreases approximately 0.57% when the oxygen flow rate decreases under CC_O_2. The product exergy shows its dynamic evolution, as presented in Figure 3(d) because it is related to the dynamic performances

DOI: 10.1021/acs.est.6b04096
Environ. Sci. Technol. 2017, 51, 725−732

of the steam and flue gas. The steam flow rate and temperature increase at the beginning of the process and then decrease to a new steady state; however, the CO_2 concentration in the flue gas decreases linearly due to robust control actions from CC_O_2. From the interactions of fuel and product exergies, exergy destruction increases slightly and exergy efficiency decreases slightly. For the same reason as presented in the above two cases, different dynamic exergy properties between closed-loop and open-loop controls are obtained and explained in Text S4.

3.5. Energy Consumption for Operating Scenario. Calculated from eq 2, Table 1 lists the energy consumption for the oxy-combustion boiler island with different control structures during the flow rate change process. Energy consumption in **O** is the greatest and is larger than those in other control systems. These results imply that system inefficiency is mainly determined by the inherent properties including process flow structure and equipment performance. Although energy consumption in **R** is the least, it deteriorates system operation because its steam temperatures and flue gas O_2 content deviate from their set points. The negative value for energy consumption in the closed-loop control structure demonstrates that the control structure can save energy to improve system thermodynamic performance during the flow rate change process. The regulatory control layer saves 224.10 MW·h of energy, while 37.96 MW·h of energy is consumed in the supervisory control layer to push steam temperatures and oxygen content in flue gas back to their set points to ensure safe and stable operation. Considering different control loops in the supervisory control layer, it is found that the energy consumption distribution ranks as follows: TC_SH (67.01%) > TC_RH (16.64%) > ratio controls (10.64%) > CC_O_2 (5.89%). Energy consumption in the steam temperature controls accounts for 83.65% of the total energy consumption caused by the supervisory control layer, which indicates that steam temperature controls are particularly important for an oxy-combustion boiler island and should be observed during operations. An interesting finding is that the sum of energy consumptions for different control loops in the supervisory control layer is unequal to and 18.69% larger than that of the corresponding simulation result. These results are attributed to cross arrangements between the reheaters and superheaters configured in the furnace in which their temperature controls regulating spray water have a positive correlation. Therefore, the cooperative effect reflected on the energy performance of TC_SH and TC_RH shows that 7.10 MW·h is saved.

Table 1. Energy Consumptions for Different Control Structures under the Flow Rate Change Process

control structure	φ, MW·h	control structure	$\Delta\varphi$, MW·h
C	7470.05	regulatory control layer	−224.10
RR	7436.80	supervisory control layer	37.96
RSH	7466.99	TC_SH	30.20
RRH	7444.30	TC_RH	7.50
RC	7439.45	CC_O_2	2.65
R	7432.09	ratio controls	4.71
O	7656.19	supervisory control layer[a]	45.06
		closed-loop control structure	−186.14

[a]Calculated from the sum of control loops in the supervisory control layer.

Table S3 summarizes the energy performance for an oxy-combustion boiler island during three operating cases. Due to the oxygen purity, the combustion process enhancement, and the flue gas CO_2 concentration, the maximum energy inputs and outputs are presented in the oxygen purity change case under closed-loop control. Among three operating conditions, the flow rate change case shows the most efficient thermodynamic performance. The maximum energy utilization ratio is ascribed to the easily realized flow controls. Comparing the closed-loop and open-loop controls, the energy utilization ratios in the flow rate and oxygen purity change cases are higher; however, the utilization ratio in the air in-leakage case is lower. Therefore, the control system is energy saving for flow rate and oxygen purity change cases, while energy is consumed during the air in-leakage change process.

3.6. Sensitivity of Operating Parameter. To investigate the sensitive degree of the operating parameters on system operation, sensitivity factors for three operating cases are determined from eq 3. From Table 2, the sensitivity factors rank as follows: oxygen purity change > flow rate change > air in-leakage change. This ranking indicates that the oxygen purity variation makes system performance more sensitive than that of flow rate and air in-leakage. In the oxygen purity change case, the unit oxygen purity variation contributes to approximately 23.89 times greater energy consumption because larger influences on oxygen, spray waters, steams, and flue gas exergies are caused. Although air in-leakage in the furnace increases the CPU energy consumptions where the CO_2 concentration in the flue gas decreases, little influence on the oxy-combustion boiler island energy consumption is observed. Compared with sensitive factors in the closed-loop and open-loop controls during an identical case, the control system presence does not affect the operating parameter identification that leads to larger system operation variation.

Table 2. Sensitivity Factors for Three Operating Scenarios

	β	
case	open-loop	closed-loop
flow rate change	4.465	4.369
oxygen purity change	23.892	23.746
air in-leakage change	1.997	2.002

3.7. Control Penalty and Control Cost. The total energy consumptions, control penalties, and control costs for three operating cases are obtained and presented in Table 3. The total energy consumptions in the oxygen purity change process are the greatest, while the minimum consumption occurs in the flow rate change process. This consumption results from the easy implementation of control actions and large influences on the oxygen, spray waters, steams, and flue gas exergies in the latter case. Identical to the predicted results when comparing the energy utilization ratios, the control system leads to 20.34 MW·h more energy consumptions in the air in-leakage change

Table 3. Energy Consumptions, Control Penalties, and Control Costs for Three Operating Scenarios

energy consumption, MW·h	open-loop	closed-loop	$\Delta\varphi$	k
flow rate change	7656.19	7470.05	−186.14	0.007
oxygen purity change	8804.36	8777.35	−27.00	0.287
air in-leakage change	8755.22	8775.56	20.34	0.099

DOI: 10.1021/acs.est.6b04096
Environ. Sci. Technol. 2017, 51, 725−732

process, while the system contributes to 186.14 MW·h and 27.00 MW·h energy savings for the flow rate and oxygen purity change processes, respectively. These results imply that system properties and disturbance types determine which influence (beneficial or harmful) the control system plays when the interference causes operational deviation. For control costs, the order is as follows: oxygen purity change > air in-leakage change > flow rate change. Small control efforts are required during the flow rate change process because minimal control actions are required to obtain the desirable steam temperatures and flue gas O_2 content. However, to maintain the operating targets in the oxygen purity change case, tighter control signals should be sent to the corresponding actuators. Thus, more attention should be paid to oxygen purity change to guarantee safe and robust operation.

During the flow rate change process, important levels of control layers and loops are uncovered according to their control costs as presented in Table 4. The required control efforts to maintain different operating goals are distinctive and depend on the types of controlled operating parameters. Moreover, controlling all operating targets simultaneously is more effective because it requires smaller control costs than controlling a single operating target. For control layers and loops, the supervisory control layer and ratio controls are more important during the flow rate change case because of the greater control costs.

Table 4. Control Costs for Different Control Structures during the Flow Rate Change Process

control system	k	control structure	k
C	0.0069	regulatory control layer	0.4753
RR	0.9713	supervisory control layer	0.5014
RSH	0.9753	TC_SH	0.0040
RRH	0.9723	TC_RH	0.0010
RC	0.9717	CC_O_2	0.0004
R	0.4753	ratio controls	0.4960

In summary, the proposed dynamic exergy method offers a new approach to identify the control impacts and achieve thermodynamically efficient operation for an energy conversion system. The method can be used to observe the real-time thermodynamic behavior, determine the utilization extent of energy, identify the operating parameter sensitivity levels, and quantify the control influences and control efforts for system operation. When applied to the complex oxy-combustion boiler island system, the proposed method is helpful and effective in realizing the expected goals. Dynamic exergy properties and energy performances of the control system are related to the operating condition, while system operation is most efficient during the flow rate change process and most sensitive to the oxygen purity variation. More control efforts should be implemented to address oxygen purity changes. Energy consumption and large control costs are required by the supervisory control layer to maintain operating targets. Steam temperature controls contribute to the main energy consumption, while ratio controls require the largest control efforts in the supervisory control layer. Further research would be embedding the environmental factor into the current approach for forming a dynamic exergoenvironmental analysis method to reduce the environmental impacts in real-time and locating the exergy destruction in devices to provide more information for monitoring their real-time performance.

■ ASSOCIATED CONTENT

Supporting Information

The Supporting Information is available free of charge on the ACS Publications website at DOI: 10.1021/acs.est.6b04096.

Texts S1−S4; Tables S1−S3; Figures S1−S3 (PDF)

■ AUTHOR INFORMATION

Corresponding Author

*Phone: +86 27 8754 2417 x8208. Fax: +86 27 8754 5526. E-mail: klinsmannzhb@163.com.

ORCID

Haibo Zhao: 0000-0003-4700-4933

Zhiwu Liang: 0000-0003-1935-0759

Notes

The authors declare no competing financial interest.

■ ACKNOWLEDGMENTS

This work was supported by The National Natural Science Foundation of China (grant nos. 51522603 and 51390494) and The Fundamental Research Funds for the Central Universities.

■ REFERENCES

(1) Dincer, I. The role of exergy in energy policy making. *Energy Policy* **2002**, *30* (2), 137−149.

(2) Dewulf, J.; Van Langenhove, H.; Muys, B.; Bruers, S.; Bakshi, B. R.; Grubb, G. F.; Paulus, D.; Sciubba, E. Exergy: its potential and limitations in environmental science and technology. *Environ. Sci. Technol.* **2008**, *42* (7), 2221−2232.

(3) Bejan, A.; Tsatsaronis, G.; Moran, M. *Thermal design & optimization*; John Wiley & Sons: New York, 1996.

(4) Li, S.; Jin, H.; Gao, L.; Mumford, K. A.; Smith, K.; Stevens, G. Energy and Exergy Analyses of an Integrated Gasification Combined Cycle Power Plant with CO_2 Capture Using Hot Potassium Carbonate Solvent. *Environ. Sci. Technol.* **2014**, *48* (24), 14814−14821.

(5) Lozano, M.; Valero, A. Theory of the exergetic cost. *Energy* **1993**, *18* (9), 939−960.

(6) Tsatsaronis, G. Thermoeconomic analysis and optimization of energy systems. *Prog. Energy Combust. Sci.* **1993**, *19* (3), 227−257.

(7) Jin, B.; Zhao, H.; Zheng, C. Thermoeconomic cost analysis of CO_2 compression and purification unit in oxy-combustion power plants. *Energy Convers. Manage.* **2015**, *106* (2015), 53−60.

(8) Zhang, C.; Chen, S.; Zheng, C.; Lou, X. Thermoeconomic diagnosis of a coal fired power plant. *Energy Convers. Manage.* **2007**, *48* (2), 405−419.

(9) Xiong, J.; Zhao, H.; Zhang, C.; Zheng, C.; Luh, P. B. Thermoeconomic operation optimization of a coal-fired power plant. *Energy* **2012**, *42* (1), 486−496.

(10) Hau, J. L.; Bakshi, B. R. Expanding exergy analysis to account for ecosystem products and services. *Environ. Sci. Technol.* **2004**, *38* (13), 3768−3777.

(11) Alanya, S.; Dewulf, J.; Duran, M. Comparison of Overall Resource Consumption of Biosolids Management System Processes Using Exergetic Life Cycle Assessment. *Environ. Sci. Technol.* **2015**, *49* (16), 9996−10006.

(12) Dincer, I.; Rosen, M. A. Exergy as a driver for achieving sustainability. *Int. J. Green Energy* **2004**, *1* (1), 1−19.

(13) Petrakopoulou, F.; Tsatsaronis, G.; Morosuk, T. Advanced exergoenvironmental analysis of a near-zero emission power plant with chemical looping combustion. *Environ. Sci. Technol.* **2012**, *46* (5), 3001−3007.

(14) Luyben, W. L.; Tyreus, B. D.; Luyben, M. L. *Plantwide process control*; McGraw-Hill: New York, 1998; pp 1−391.

(15) Munir, M.; Yu, W.; Young, B. Plant-wide control: Eco-efficiency and control loop configuration. *ISA Trans.* **2013**, *52* (1), 162−169.

DOI: 10.1021/acs.est.6b04096
Environ. Sci. Technol. 2017, 51, 725−732

(16) Munir, M. T.; Yu, W.; Young, B. R. Dynamic exergy plots using exergy factor. *Trans. Control Mech. Syst.* **2012**, *1* (1), 13−19.
(17) Jin, B.; Zhao, H.; Zheng, C. Dynamic exergy method and its application for CO_2 compression and purification unit in oxy-combustion power plants. *Chem. Eng. Sci.* **2016**, *144* (2016), 336−345.
(18) Buhre, B. J. P.; Elliott, L. K.; Sheng, C. D.; Gupta, R. P.; Wall, T. F. Oxy-fuel combustion technology for coal-fired power generation. *Prog. Energy Combust. Sci.* **2005**, *31* (4), 283−307.
(19) Mousavian, S.; Mansouri, M. T. Conceptual feasibility study of retrofitting coal-fired power plant with oxy-fuel combustion. *Proc. Inst. Mech. Eng., Part A* **2011**, *225* (6), 689−700.
(20) Xiong, J.; Zhao, H.; Zheng, C. Exergy analysis of a 600 MWe oxy-combustion pulverized-coal-fired power plant. *Energy Fuels* **2011**, *25* (8), 3854−3864.
(21) Mansouri, M. T.; Mousavian, S. Exergy-based analysis of conventional coal-fired power plant retrofitted with oxy-fuel and post-combustion CO_2 capture systems. *Proc. Inst. Mech. Eng., Part A* **2012**, *226* (8), 989−1002.
(22) Jin, B.; Zhao, H.; Zou, C.; Zheng, C. Comprehensive investigation of process characteristics for oxy-steam combustion power plants. *Energy Convers. Manage.* **2015**, *99* (2015), 92−101.
(23) Xiong, J.; Zhao, H.; Zheng, C. Techno-economic evaluation of oxy-combustion coal-fired power plants. *Chin. Sci. Bull.* **2011**, *56* (31), 3333−3345.
(24) Jin, B.; Zhao, H.; Zheng, C. Dynamic modeling and control for pulverized-coal-fired oxy-combustion boiler island. *Int. J. Greenhouse Gas Control* **2014**, *30* (2014), 97−117.
(25) Jin, B.; Zhao, H.; Zheng, C. Dynamic simulation for mode switching strategy in a conceptual 600MWe oxy-combustion pulverized-coal-fired boiler. *Fuel* **2014**, *137* (2014), 135−144.
(26) Luyben, W. *Plantwide dynamic simulators in chemical processing and control*; CRC: New York, 2002; p 448.
(27) Jin, B.; Zhao, H.; Zheng, C. Optimization and control for CO_2 compression and purification unit in oxy-combustion power plants. *Energy* **2015**, *83* (2015), 416−430.
(28) Jin, B.; Su, M.; Zhao, H.; Zheng, C. Plantwide control and operating strategy for air separation unit in oxy-combustion power plants. *Energy Convers. Manage.* **2015**, *106* (2015), 782−792.
(29) Gaggioli, R.; Petit, P. J. Use the second law, first. *CHEMTECH (United States)* **1977**, *7* (8), 496−506.
(30) Verda, V.; Serra, L.; Valero, A. The effects of the control system on the thermoeconomic diagnosis of a power plant. *Energy* **2004**, *29* (3), 331−359.

DOI: 10.1021/acs.est.6b04096
Environ. Sci. Technol. 2017, 51, 725−732